

Electrochemical Rutin Sensor Based on Graphene Oxide and Functionalized Multiwall Carbon Nanotubes@nafion_{0.1%} Hybrid Nanocomposite modified glassy carbon electrode

Praveen Kumar G¹, Raja Nehru¹, Shen-Ming Chen^{1*}, Bandar Mohsen Almunqedhi², Tse-Wei Chen^{1,3}, Jun-Yu Wang¹, Ming-Chin Yu^{4,*}, Noura M. Darwish⁵

¹ Department of Chemical Engineering and Biotechnology, National Taipei University of Technology, Taipei 10608, Taiwan.

² Department of Botany and Microbiology, College of Science, King Saud University, P.O. Box 2455, Riyadh 11451, Saudi Arabia.

³ Research and Development Center for Smart Textile Technology, National Taipei University of Technology, Taipei 106, Taiwan, ROC.

⁴ Department of Surgery, Chang Gung Memorial Hospital, Taoyuan 333, Taiwan (R.O.C)

⁵ Biochemistry Department, Ain Shams University, Dokki, Cairo 12311, Egypt.

*E-mail: smchen78@ms15.hinet.net(Shen-Ming Chen), mingchin2000@gmail.com(Ming-Chin Yu)

Received: 5 March 2019 / Accepted: 16 April 2019 / Published: 10 June 2019

A highly sensitive electrode based on graphene oxide and functionalized multiwall carbon nanotube hybrid composite as coated on glassy carbon electrode (GCE) for the electrochemical rutin sensor. The as-prepared GO/*f*-MWCNTs@nafion composite was characterized by promising analysis such as field emission scanning electron microscopy (SEM), energy-dispersive X-ray spectroscopy (EDX), Fourier transform infrared spectroscopy (FT-IR), X-ray photoelectron spectroscopy (XPS), UV-Vis Diffusive reflectance spectroscopy (UV-DRS). The GO/*f*-MWCNTs@nafion/GCE hybrid nanocomposite revealed substantial electrocatalytic activity toward the rutin sensor. The GO/*f*-MWCNTs@nafion/GCE electrode manifested voltammetric response over the concentration ranging of 0.02 to 39.69 μ M with a limit of detection (LOD) 0.004 nM, respectively. This analytical values suppressed the previously existing method for the electrochemical sensing of rutin. Additionally, the modified electrode proposed excellent stability, repeatability, and sensitivity.

Keywords: Flavonoid, Antioxidant, GO, *f*-MWCNTs, Hummer's method, and stability.

1. INTRODUCTION

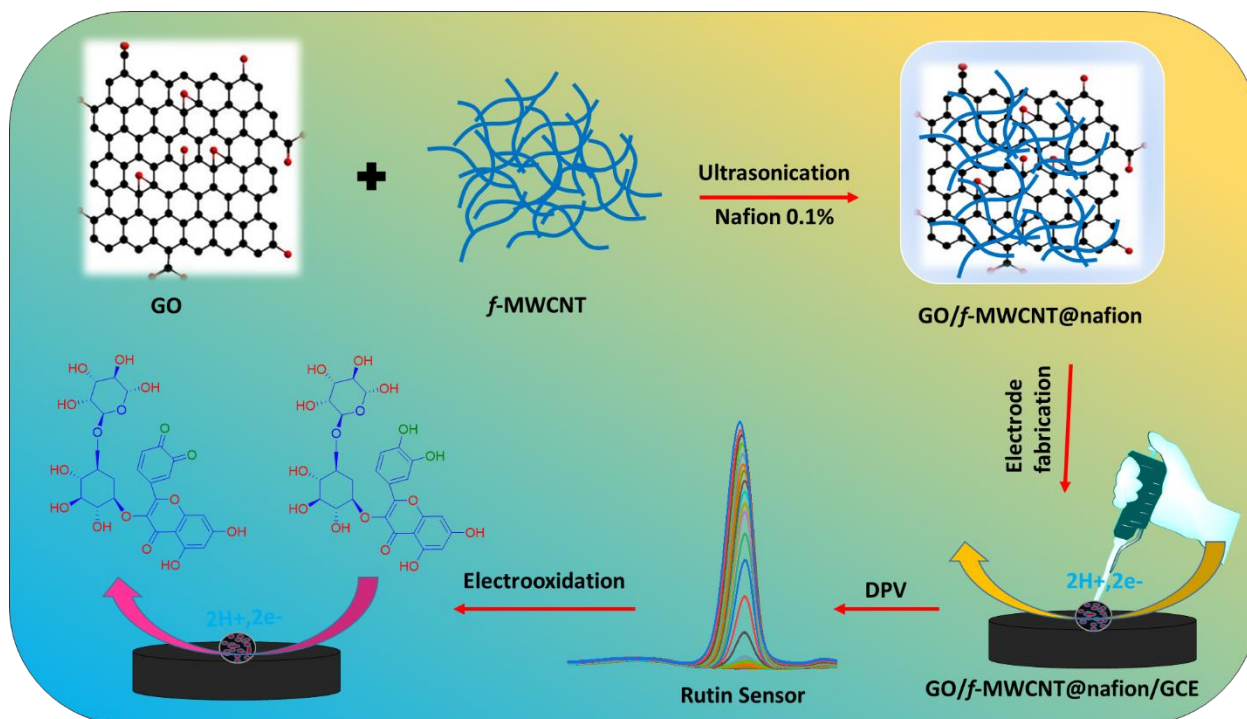
Rutin (nutrient P) is also the flavonoid glycoside component which is commonly present in several species of the plant [1]. Besides, its usage covers an extensive range of different industrial sectors such as food, beverage, pharmaceutical, personal care and clinical due to its antioxidant

properties. In the biological term, it also helps in promoting specific body functions beyond the scope of basic needs of nutrition or vitamin [2, 3]. Although, it's various health beneficiary applications as medicine for cancer, inflammation, and also stop oxidations [4-9]. These can generate severe health problems for living beings. While consuming overdosage of rutin creates headaches, flushing, rashes, or stomach upset and especially it affects breastfeeding. Thus, the prime determination of rutin in the ecosystem is necessary. UV-visible spectrometry[10], HPLC chromatography[11], capillary electrophoresis[12] and chemiluminescence[13] are the various methods have been introduced to detect the presence of rutin.

Among these methods, the electrochemical analysis is a straightforward, less expensive, portable and rapid technique [14]. Hence, in this study, the electrochemical approach has been utilized for the detection of rutin. In this case, to improve the strength, selectivity, affectability and hostile to surface fouling properties of the electrode, finding an appropriate, significantly advanced electrode material is necessary [15].

Graphene is a sheet-like structure exfoliate from graphite and it is sp^2 hybridized carbon molecules in the hexagonal plan. Since graphene been used for various applications in recent research, it is denoted to be a "rising star" in science and technology [16, 17]. Due to its flexibility towards the structure, it can be tuned up to different structure which can be functionalized for different application. For example, graphene can be stacked into MWCNTs and rolled up to CNTs and even turned to Buckyball (fullerene) they all play their unique role in science. As it has wide properties such as a controllable band gap, huge surface to volume ratio, electrical and thermal conductivity, they can be blindly applied in different areas such as photocatalyst, electronics system, sensors, medicine, supercapacitors and solar cells [18].

As we know carbon-based materials are the most conductive and abundant material. Particularly, carbon nanotubes are the most interesting topic in recent eras due to their wide properties such as good conductivity, flexibility, and a major source for extensive applications such as supercapacitor, batteries, fuel cell, and sensors. From the group of carbon, carbon nanotube (CNT) a barrel - shaped structure with tail end porous. Since it has a high surface area, good electrical conductivity, thermal, mechanical and stable property, the MWCNTs are utilized in different energy and photonic applications. In addition, during the functionalization process, the MWCNT obtains the larger catalytic activities towards the target. On the other hand, graphene oxide is also said to be a carbon-based material that has superior conductivity and physiochemical properties. Hence, it used extensively in different applications like photocatalytic, energy storage, catalyst, an electrochemical sensor. Hence, the GO and CNTs tend to prepare the composite for GCE to determine the analyte-rutin. Here, we discuss the synthesis of a crumpled GO/*f*-MWCNTs@nafion composite by particular methods and the composite was prepared by ultra-sonication. The as-synthesized material was used to deposit on GCE and the electrochemical sensing of rutin has been carried out. The complete application of this pharma sensor shows a clear picture of the detection, quantity and quality measurements of the drug rutin and it's potential. Further the functionalized electrode's capabilities have been analyzed using DPV.



Scheme 1. Schematic illustration of electrochemical rutin sensor based on GO and *f*-MWCNTs

2. EXPERIMENTAL SECTION

2.1 Materials and methods

Graphite powder, carbon nanotubes (MWCNTs), sodium hydroxide (NaOH) were all in analytical grade and obtained from Sigma-Aldrich. The PB solution of pH-3 (0.05 M) was prepared from (NaH_2PO_4) and (Na_2HPO_4), which was subsequently used for electrochemical experiments. The complete experiment was carried out using DI water (De-Ionized).

Scanning electron microscope analysis done to study the morphological structure of the composite using (FE-SEM) JEOL-7600F device. Fourier transform infrared spectroscopy (FT-IR) JASCO CHI 1000C FT/IR-6600 instrument used to analyze the functional group elements present in the composite. Energy-dispersive X-ray spectroscopy (EDX) attached HORIBA EMAX X-ACT is used to analyze the percentage of an element in the composite. (CHI 1205c) the cyclic voltammetry device used for the electrochemical experiments to determine the rutin, an analyte for this complete work. In general, it is a three electrode system. Where, GCE, platinum wire and Ag/AgCl (sat. KCl) were used in the three electrode system.

2.2 Synthesis of GO/*f*-MWCNTs@nafion nanocomposite

The typical modified Hummer's technique was used to prepare graphene oxide from the commercial graphite powder. Briefly, 2 g of graphite powder and 8 g of KMnO_4 were added into the

beaker containing 100mL of Con. Sulphuric acid. This mixture then places into the ice bath with rapid stirring for 2 h. The temperature of the bath was maintained up to 10 °C. Thereafter the ice bath was removed and the beaker with the mixture was changed into the water bath by maintaining the temperature at 35 °C for 1 h under continuous stirring. Then the mixture was weakening by adding 100 mL of DI water and stirred for 1h. Followed by the mixture was further dissolved with 300 mL of de-ionized water. Afterward, 20mL of 30% H₂O₂ was added to diminish the residual KMnO₄ (the color changes from brown residue to brilliant yellow). Then the obtained precipitate washed with a 5% HCl solution and copious amount of distilled water to neutralize the mixture. Finally, the obtained solid was dried at 60°C for 24h and denoted as GO.

The CNTs are allowed to be functionalized on the surface. The functionalized carbon nanotube (*f*-MWCNTs) obtain a high surface-volume ratio area. Therefore, -COOH and -OH were functionalized on MWCNTs surface according to the literature. Briefly, the pure-MWCNTs (0.5 g) was stirred in 50 mL (1: 1 v/v) ratio of HNO₃ (67%) and H₂SO₄ (97%) and placed under 60°C for 30 min under constant stirring. Then, the mixture was allowed to sonicate around 5-6 h and finally, the temperature reduces to atmospheric temperature. The *f*-MWCNTs precipitate is washed by centrifuging to separate the unreacted acids using DI water. This procedure followed for several times until it reaches the pH 7, shows the material is neutral. The obtained precipitate of *f*-MWCNTs is allow dried at open air temperature. The functionalized carbon nanotube and GO materials were measured and allowed for the water bath ultra-sonication approach at room temperature for 1 h to obtain well-dispersed composite.

2.3. Fabrication of GO/*f*-MWCNTs@nafion modified hybrid electrode.

The GO/*f*-MWCNTs composite material was weighed and allowed to disperse in distilled water with 0.1% Nafion and sonicated to get the homogeneous suspended solution. About 6 μL of suspension was dispersed on a well-polished GCE surface and allow to dry for few minutes. Afterward, the GO/*f*-MWCNTs@nafion nanocomposite modified GCE used for the electrochemical experiments.

3. RESULT AND DISCUSSION

3.1. FT-IR, UV-visible spectroscopy

The active components of the synthesized materials were studied by Fourier transmission infrared (FT-IR) spectra. Fig.1 (a) explains the FTIR spectra of the (a) GO/*f*-MWCNTs, whereas, the peaks 1000 to 3000 are weak absorption peaks and peak at 3440 cm⁻¹ are strong absorption peaks. The different peaks 1062 shows C-O, 1404 shows C=C and 1720 cm⁻¹ has C=O stretching vibrations of the GO. Also, the peaks at 2902 and 2980 cm⁻¹ were showed the symmetric and asymmetric CH₂ stretching vibrations of the GO/*f*-MWCNTs@nafion. The presence of the hydroxyl group in composite GO/*f*-MWCNTs@nafion shows at 3440 cm⁻¹ [19]. Fig. 1(b), shows the UV-visible spectra of GO/*f*-

MWCNT, here the peak at 266 nm is because of the π - π^* stacking interaction transition in GO/f-MWCNTs@nafion composite [19]. This study confirms that the material has been synthesized as GO/f-MWCNTs@nafion composite.

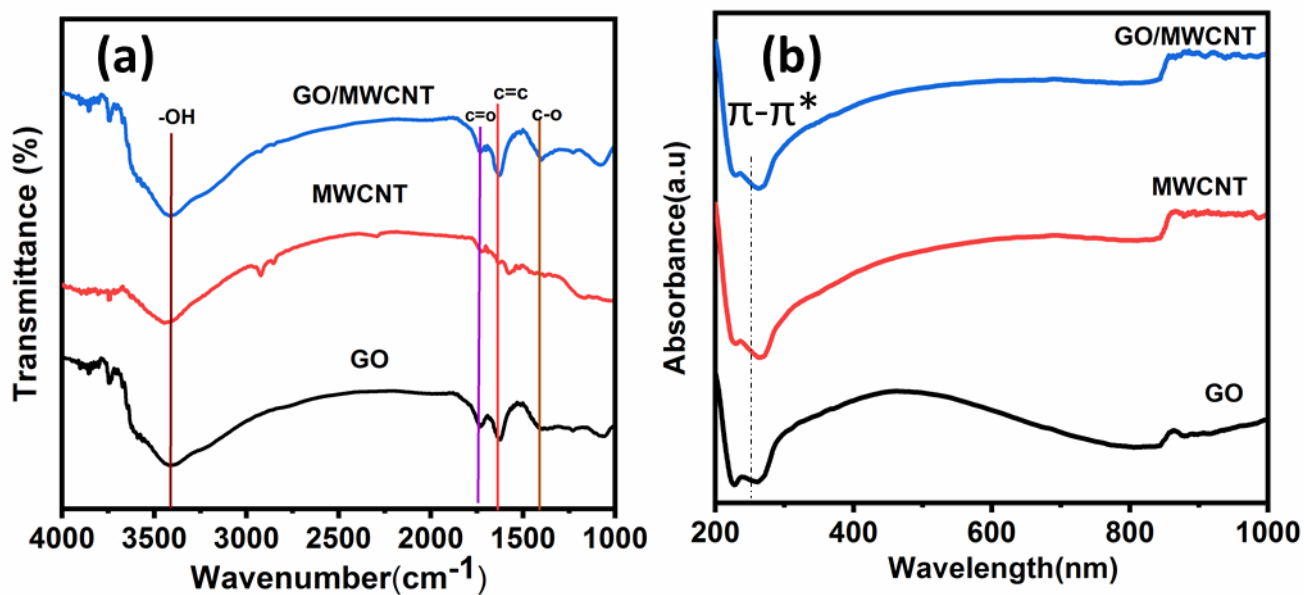


Figure 1. (a) Shows the FT-IR spectra for both material and composites (b) predicts the UV-Visible DRS spectra for the as-prepared material and composite.

3.2. Structural and morphology of GO/f-MWCNTs

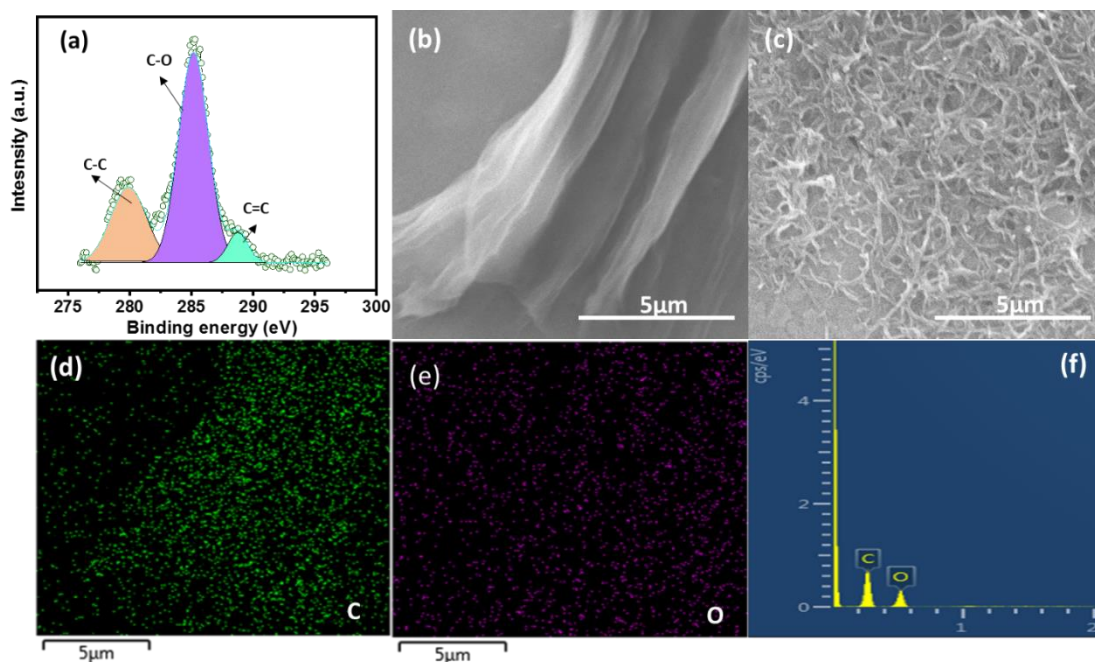


Figure 2. (a) XPS of the structured composite, (b) and (c) SEM image of the synthesized materials GO and GO/f-MWCNTs. (d) and (e) predicts the volume of carbon and oxygen. (f) Shows the percentage of both carbon and oxygen element present.

The morphology of the material was investigated by scanning electron microscope (SEM) shown in Fig.2. Fig.2 (b and c) shows the SEM images of GO/f-MWCNTs@nafion shows that the tube was dispersed on the crumpled sheets. This is due to the π - π stacking interaction among the side walls of f-MWCNT and GO sheets [20]. For further clarification, XPS was also carried out to know the elements present at certain valance state. Fig.2 (a) portrays clearly that C-C, C-O, and C=C are formed at particular peaks, which confirms as-synthesized material [21]. Fig. 2(d and e) gives complete knowledge about mapping where the quantitative image shows the amount of carbon and oxygen present. Moreover, the number of elements present in the composite GO/f-MWCNTs@nafion was shown in Fig.2 (e). The Energy dispersive x-ray spectrum obtained gives the carbon and oxygen signals that confirm the oxidized graphene and the carbon.

3.3. Electrocatalytic Redox reaction of Rutin at modified GCE

Cyclic voltammetry analysis carried out to analyze the electrocatalytic activity of the modified surface by determining the rutin in 0.05M PB solution (pH 3) at 50 mVs⁻¹. By adding 200 μ M rutin, the electrocatalytic activity of the bare GCE (a), GO/f-MWCNTs@nafion/GCE (b), was checked and the obtained CV results are shown in Fig.3 (a). The bare GCE shows a higher oxidation peak potential of 0.58 V and the inferior anodic peak current due to its poor active sites. However, the GO/f-MWCNTs@nafion/GCE oxidizes rutin shows a reduction and the oxidation peak's current value increased due to the large surface area. The GO/f-MWCNTs@nafion/GCE exhibited an improved electrocatalytic activity with a pronounced signal increment in the oxidation peak current to about 10.55 μ A, which is higher than the other modified electrodes. The enhancement in the electrochemical performance of the GO/f-MWCNTs@nafion/GCE towards rutin oxidation was due to the combination of two unique nanomaterials that have a large surface area and excellent catalytic activity. For a clear view, the CV images of the bare GCE (a), GO/f-MWCNTs@nafion/GCE (b), are displayed in Fig.3 (a). To determine the influence of pH for rutin over the GO/f-MWCNTs@nafion/GCE, different pH (3–11) values were investigated by CV and the results are presented in Fig.3 (b).

The peak current and peak potential values obtained versus the different pH of the electrolyte Fig.3(c) and (d). It is understood that the current value decreased in the pH order (3 > 5 > 7 > 9 > 11) and the peak potentials were shift to negative .This shows the exact proton reaction and concluded that pH 3 is acceptable for the determination of rutin. There is a linear relationship between pH and peak potential. The obtained slope value is around 56 mV per pH, which is close to the Nernstian value of 59 mV per pH unit.

Further, the oxidation mechanism in the electrochemical determination of rutin is well explained in Scheme 2. In this mechanism, the hydroxyl groups present in the catechol element of rutin undergo a reversible Redox reaction, producing an ortho-quinone derivative. Hence, the electrochemical oxidation of rutin at the GO/f-MWCNTs@nafion/GCE is an equall electron-proton reaction. [20, 22].

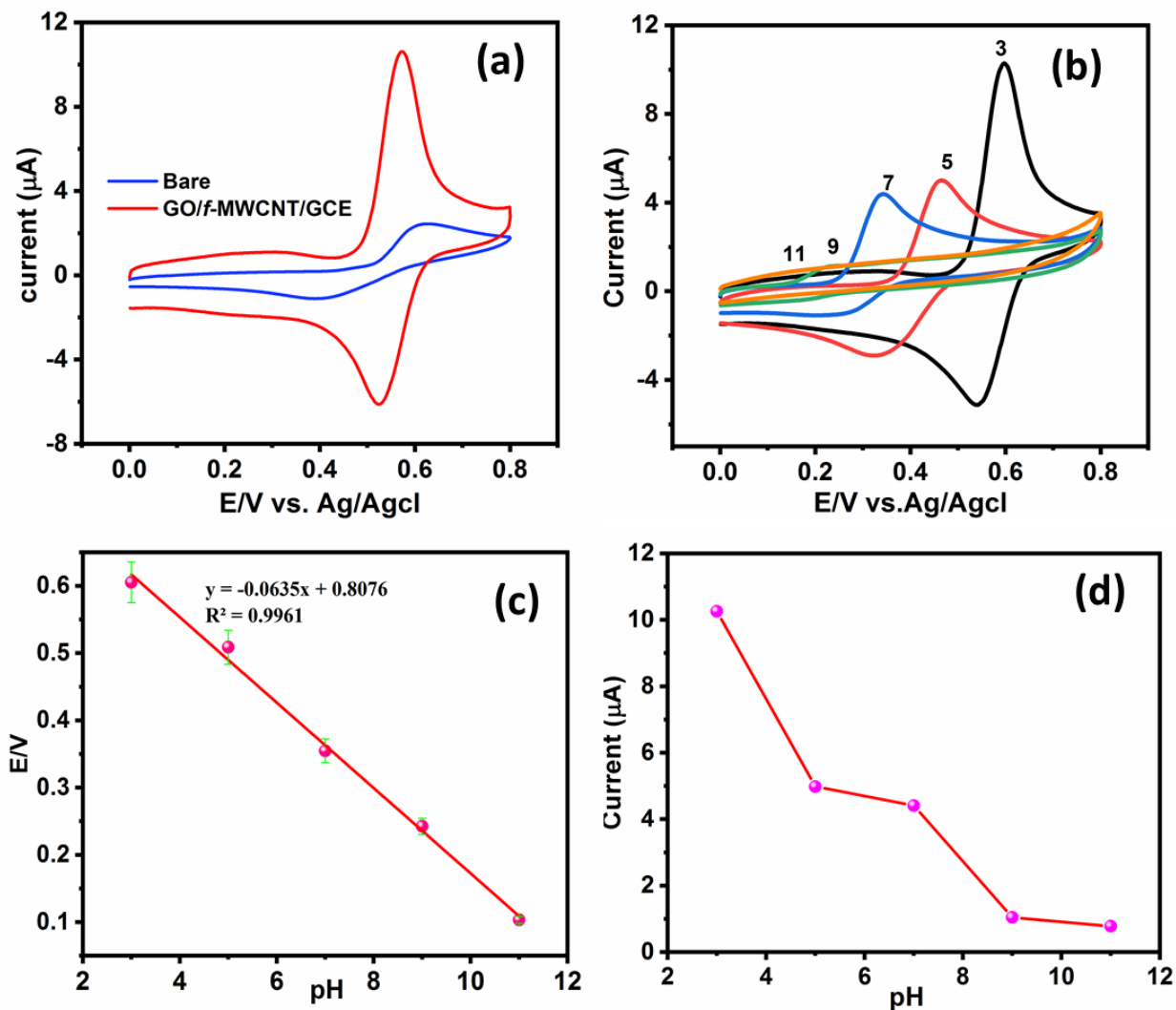
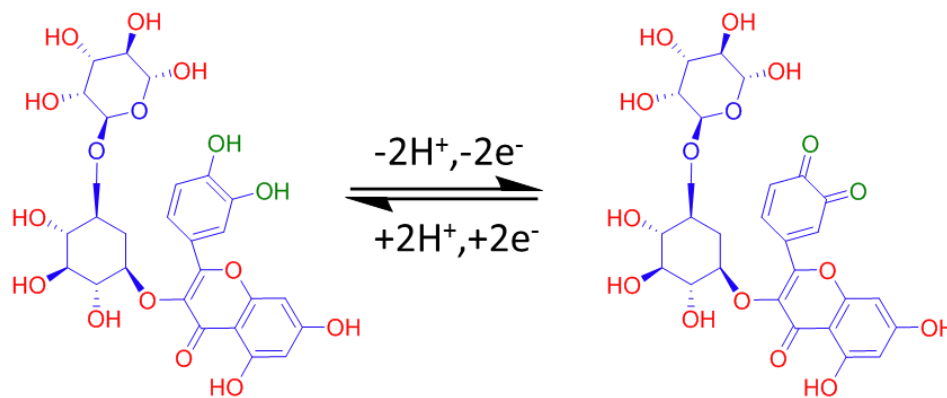


Figure 3. (a) Comparison between the bare and the modified hybrid electrode, whereas the modified GCE shows a greater response than the bare GCE. (b) Different pH for the Modified electrode, which shows changes in the current. (c) Shows pH (vs) potential and (d) pH (vs) current values.



Scheme 2. Redox mechanism of Rutin during electrochemical reaction on a modified hybrid electrode.

3.4. Effect of concentration and scan rate

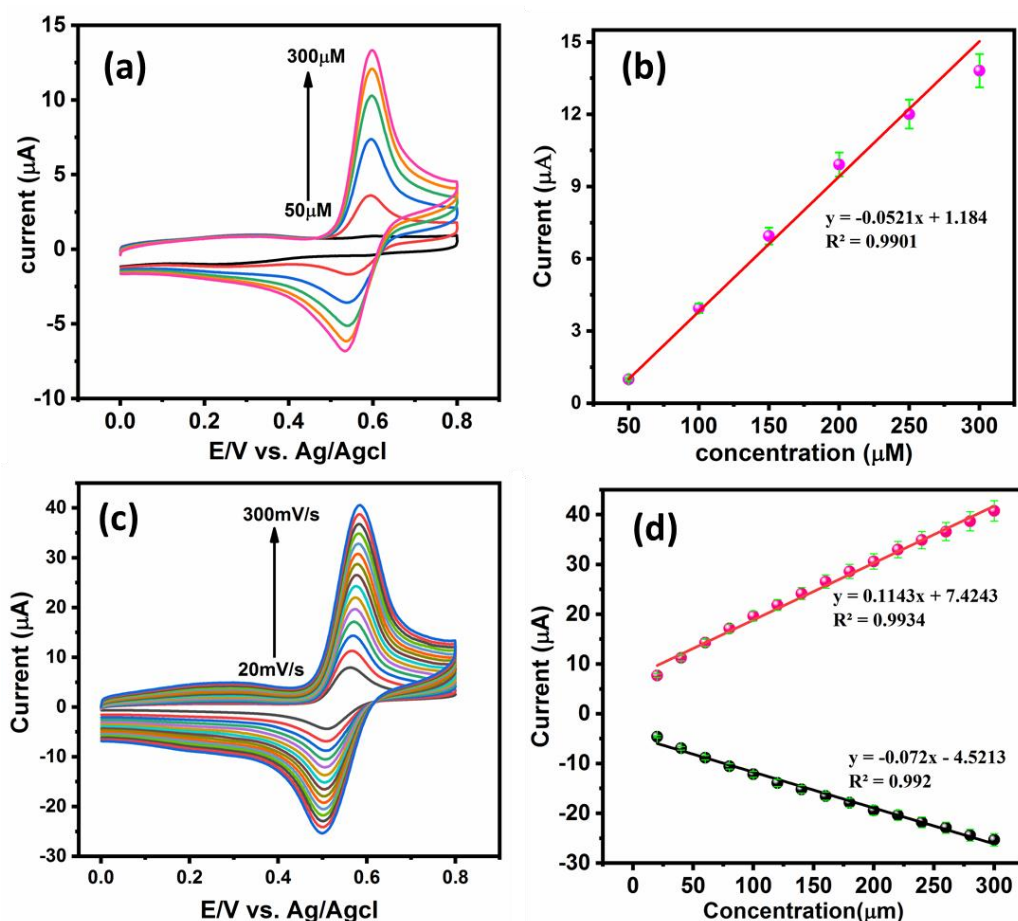


Figure 4.(a) Addition of analyte versus the current. (b) Shows a linear increase in the rate of current. (c) exhibits the different scan rate versus current rate and (d) its linear plot towards the current.

Furthermore, a different number of concentrations of rutin from 30 to 200 μM were added to the GO/*f*-MWCNTs@nafion/GCE in 0.05 M phosphate buffer solution. Fig.4 (a) exhibits the CV images of the different addition experiments, where the oxidation peak and the current were increasing for each addition of rutin. Fig.4 (b) shows the linear current increases with increasing concentration. This indicates that the modified hybrid electrode is obtaining good electrocatalytic activity. To evaluate the scan rate significance on the electro-oxidation of rutin, the investigation carried out in 0.05 M PB solution at the GO/*f*-MWCNTs/GCE. Fig.4(c), shows the scan rate from 20 to 200 mV s^{-1} for the addition of rutin 200 μM . Whereas, anodic and cathodic peak currents increase by increasing scan rates. However, these increased peak values show a linear relationship with the scan rates Fig.4 (d). And also, a shift was seen in both the peak potential, which is falling towards the +ve and -ve direction. This output explains that rutin's electro-oxidation at the GO/*f*-MWCNTs@nafion/GCE is a surface-controlled technique [23].

3.5. Determination of Rutin

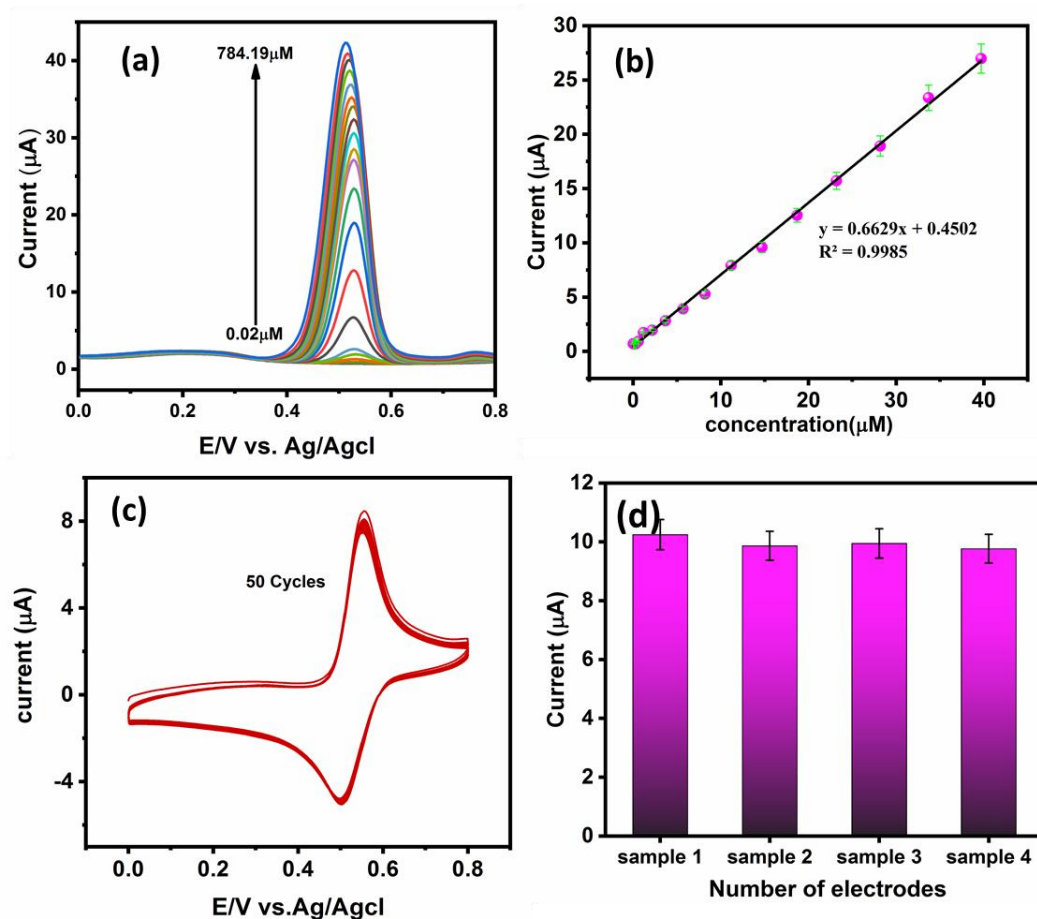


Figure 5. (a) Diffusive Potential Voltammetry (DPV) response of GO/f-MWCNTs@nafion/GCE with various concentrations of rutin in 0.05 M PBS (pH 3) from 0.002 μM to 784.19 μM . (b) The plots of the linear current of rutin vs. its concentration. (c) Proves the number of cycles of the electrode and (d) reproducibility with the different number of electrodes.

Table 1. Comparative study for the analytical behavior of our modified hybrid electrode with other literature

Electrode material	Linear range (μM)	LOD (μM)	Ref
PtNPs/RGO	0.05-10	0.01	24
NiCo ₂ O ₄ /RGO	0.1-8; 8-150	0.01	25
CNT	0.08-80	0.02	26
RG/carbon ionic liquid	0.070 - 100.0	0.024	27
Acetylene black	0.02-5	0.01	28
PdPc-MWCNTs-Nafion/GCE	0.1-51	0.075	29
CeO ₂ -modified gold electrode	0.5- 500	0.2	30
Chitosan/graphene/GCE	0.5-10.5	-	31
GO/f-MWCNTs@nafion/GCE	0.02-39.69	0.004	present Work

The electrochemical detection of rutin was studied using the DPV method at the GO/*f*-MWCNTs@nafion/GCE and the interpolated images are represented in Fig.5 (a). The DPV responses were obtained for the addition of various concentrations of rutin from 0.02 to 784.19 μM in 0.05 M PB solution. The oxidation peak current at 0.58 V was increased for the step by step addition of rutin and it exhibited a linear relationship with a coefficient of $R^2 = 0.998$ (Fig. 5b). Acceptable linearity about 0.02 to 39.69 μM , very low LOD of 0.004 μM and sensitivity is 9.2069 was acquired at the GO/*f*-MWCNTs/GCE. The literature survey showed a comparative study between the current work result obtained and published values.

(Table 1). From all these results the GO/*f*-MWCNTs@nafion/GCE shows good electrocatalytic activity. The large surface to volume ration, better flexible and extraordinary conductive property of the synthesized nanocomposite are the main source to develop the catalytic activity of this electrochemical sensor.

3.6. Stability and reproducibility

Furthermore, the effect of the Stability and reproducibility of GO/*f*-MWCNTs@nafion/GCE modified hybrid electrode were examined by CV and DPV measurement. The number of cycles has been analyzed to identify the stability of the modified hybrid electrode in the presence of 200 μM rutin as shown in Fig.5(c). In Fig.5(c) the CV response of 50 cycles, the redox current response decreases less than 5%. Fig. (5d) the reproducibility of the modified hybrid GCE was analyzed by preparing four different electrodes. It is evaluated as 2.21% which is the relative standard deviation for four different electrodes of the Rutin sensor.

4. CONCLUSION

In summary, the modified Hummer's method assisted synthesized GO, and functionalized MWCNTs turned into a composite by using a simple and eco-friendly ultra-sonication. The synthesized nanocomposite was well characterized by different methods such as SEM, EDX, XPS, FT-IR, and UV-Vis DRS and also the electrochemical impedance properties were assessed by EIS. The electrocatalytic properties of the modified electrode over rutin determination were estimated using the CV and DPV techniques. The fabricated GO/*f*-MWCNTs@nafion glassy carbon electrode exhibited superior electrochemical performance to the determination of rutin from the linear range of 0.02 to 39.69 μM with LOD 0.004 μM and high sensitivity. Additionally, the fabricated electrode possesses appreciable long term stability, repeatability, and reproducibility to the determination of rutin. Hence, we proclaim that GO/*f*-MWCNTs@nafion will be a helpful composite to design a new device to detect and act as an extraordinary sensor.

CONFLICTS OF INTEREST

There are no conflicts to declare.

ACKNOWLEDGEMENT

This project was supported by King Saud University, Deanship of Scientific Research, College of Science and Research Center. The authors are grateful for financial support (MOST 107-2113-M-027-005-MY3) from the Ministry of Science and Technology (MOST), Taiwan. The authors gratefully acknowledge the financial support of the National Taipei University of Technology and Chang Gung Memorial Hospital Joint Research Program (NTUT-CGMH-108-05) and CORPG1I0011.

References

1. K. H. Kim, K. W. Lee, D. Y. Kim, H. H. Park, I. B. Kwon, H. J. Lee. *Bioresour. Technol. Rep.*, 96 (2005) 1709–1712
2. Y. Miao, Z. Zhang, Y. Gong, Q. Zhang, G. q. Yann, *Biosens. Bioelectron.*, 52 (2014) 271–276
3. I.M. Apetreia, C. Apetreib, *Measurement* 114 (2018) 37–43
4. W. Suna, L. Dongb, Y. Lub, Y. Deng, J. Yub, X. Sunb, Q. Z. College. *Sens. Actuators, B.*, 199 (2014) 36–41.
5. J. Tao, Q. Hud, J. Yang, R. Li, X. Li, C. Lua, C. Chene, L. Wang, R. Shattock, K. Benb, *Antiviral res.*, 75 (2007) 227–233.
6. B. Hu, F. Dai, Z. Fan, G. Ma, Tang, X. Zhang *Adv. Mater.*, 27 (2015) 5499–5505.
7. R. Guo, P. Wei, *Microchim. Acta.*, 161 (2008) 233–239.
8. J. Wang, B. Yang, S. Li, B. Yan, H. Xu, K. Zhang, Y. Shi, C. Zhai, Y. Du, *J. Colloid Interface Sci.*, 506 (2017) 329–337.
9. A. Gong, W. Ping, J. Wanga, X. Zhu, *Spectrochim. Acta, Part A.*, 122 (2014) 331–336.
10. T. Z. Attia, *Spectrochim. Acta, Part A.*, 169 (2016) 82–86.
11. S. Kubendhiran, R. Sakthivel, S.M. Chen, Q. J. Yeah, B. M. and B. Thirumalraja, *Inorg. Chem. Front.*, 5 (2018), 1085.
12. Q. Wang, F. Ding, H. Li, P. He, Y. Fang, *J. Pharm. Biomed. Anal.*, 30 (2003) 1507–1514.
13. S. Li, L. Zhang, L. Chen, Y. Zhong and Y. Ni, *Anal. Methods.*, 8 (2016) 4056.
14. X.Q.Lin, J. B. Hea, Z.G. Zha, *Sens. Actuators, B.*, 119 (2006) 608–614.
15. I. M. Apetrei and C. Apetrei, *IEEE Sens. J.*, 6 (2015).
16. V. Mani, S.M. Chen, B.S. Lou, *Int. J. Electrochem. Sci.*, 8 (2013) 11641 – 11660.
17. C. N. R. Rao, A. K. Sood, R. Voggu, and K. S. Subrahmanyam. *J. Phys. Chem. Lett.*, 1 (2010) 572–580.
18. V. Mani, A.P. Periasamy, S.M. Chen, *Electrochem. Commun.*, 17 (2012) 75–78.
19. T. Kavinkumar, S. Manivannan, *J. material sci. Tech.*, 32 (2016) 626 – 632.
20. M. Liu, J. Deng, Q. Chen, Y. Huang, L. Wang, Y. Zhao, Y. Zhang, H. Li, S. Yao *Biosens. Bioelectron.*, 41 (2013) 275–281.
21. L. Zhao, X. Su, Z. Lei, J. Zhao, J. Wu, Q. Li, A. Zhang, *Compos. Part B-Eng.*, 83 (2015) 317–322.
22. R. Xing, H. Yang, S. Li, J. Yang, X. Zhao, Q. Wang, S. Liu X. Liu, *J. Solid State Electrochem.*, 21 (2017) 1219–1228.
23. K.J. Huang, L. Wang, Y.J. Liu, T. Gan, Y.M. Liu, L.L. Wang, Y.Fan. *Electrochim. Acta.*, 107 (2013) 379–387.
24. Q. Zheng, B. Zhang, X. Lin, X. Shen, N. Yousefi, Z.D. Huang, Z. Li and J.K. Kim, *J. Mater. Chem.*, 22 (2012) 25072
25. Y. Wu, C. Hu & M. Huang, N. Song, W. Hu, *Ionics.*, (2015) 21:1427–1434.
26. P. Pang, H. Li, Y. Liu, Y. Zhang, L. Feng, H. Wang, Z. Wub and W. Yangac, *Anal. Methods.*, 7 (2015) 3581.
27. S. Cuia, L. Li, Y. Dinga, J. Zhang, H. Yangb, Y., Wang, *Talanta.*, 164 (2017) 291–299.
28. L. Yan, X. Niu, W. Wang, X. Li, X. Sun, C. Zheng, J. Wang, W. Sun. *Int. J. Electrochem. Sci.*, 11 (2016) 1738 – 1750.

29. J. Song , J. Yang, J. Zeng, J. Tan, L. Zhang, *Microchim. Acta.*, 171 (2010) 283–287.
30. R. Xing, H. Yang, S. Li, J. Yang, X. Zhao, Q. Wang, S. Liu, X. Liu. *J Solid State Electrochem.* 21 (2017) 1219–1228.
31. J. Ana, Y.Y. Bia, C.X. Yanga, F.D. Hua, C.M. Wang, *J. Pharm. Anal.*, 3(2) (2013) 102–108.
32. Y. Wei, G. Wang, M. Li, C. Wang, and B. Fang, *Microchim. Acta.*, 158 (2007) 269–274.

© 2019 The Authors. Published by ESG (www.electrochemsci.org). This article is an open access article distributed under the terms and conditions of the Creative Commons Attribution license (<http://creativecommons.org/licenses/by/4.0/>).